Performance of the Split-Symbol Moments SNR Estimator in the Presence of Inter-Symbol Interference

B. Shah

Radio Frequency and Microwave Subsystems Section

S. Hinedi

Communications Systems Research Section

The Split-Symbol Moments Estimator (SSME) is an algorithm that is designed to estimate symbol signal-to-noise ratio (SNR) in the presence of additive white Gaussian noise (AWGN). This article examines the performance of the SSME algorithm in band-limited channels and quantifies the effects of the resulting inter-symbol interference (ISI). All results obtained herein are in closed form and can be easily evaluated numerically for performance prediction purposes. Furthermore, they are validated through digital simulations.

I. Introduction

The Deep Space Network Baseband Assembly (BBA) and Advanced Receiver (ARX) use a Split-Symbol Moments Estimator (SSME) algorithm to estimate the symbol signal-to-noise ratio (SNR) of the received signal. The algorithm was designed to operate in the presence of additive white Gaussian noise (AWGN) and at data rates low enough so that bandwidth limiting is insignificant. Its principle of operation relies on using the outputs of two accumulators each operating on a separate half of the same symbol. The product of the outputs provides, after av-

eraging, an estimate of the signal power. An estimate of total power is obtained by summing both accumulations, thus integrating over the full symbol period, squaring the sum, and then averaging to obtain an estimate of signal mean-square plus noise variance. By processing both these averages, an estimate of the symbol SNR can be easily derived.

This article examines the performance of the SSME when the data stream is filtered and inter-symbol interference (ISI) results. This is a likely scenario in the ARX II (current version of ARX) which has a 20-MHz processing

rate and a data rate goal of 6.6 Msymbols/sec. The ratio of the bandwidth W to the highest data rate (R_h) expected is $W/R_h = 1.33$ assuming an 8.8-MHz 3-dB telemetry bandwidth. Analysis and simulations are used simultaneously to quantify the performance of the SSME in band-limited channels. Throughout this article, perfect carrier, subcarrier, and symbol synchronization are assumed, since the purpose of the analysis is to quantify the effects of filtering only.

II. The Split-Symbol Moments Estimator (SSME)

The input to the SSME consists of a sequence of samples obtained by processing the received signal. The processing can be broken into two stages: analog and digital. In the ARX II, for instance, the received signal is first downconverted to an intermediate frequency and filtered using analog circuits. This is followed by an analog-to-digital converter after which the carrier, subcarrier, and symbol synchronization are performed digitally. It is assumed that the synchronization function is performed in an ideal fashion and is thus ignored in this article. Figure 1 depicts a basic model for the telemetry signal processing up to the SSME input. The analog filtering function is lumped into a single equivalent filter $H(s)$ and the digital processing is represented by the filter $H(z)$. Given symbol timing, the SSME estimates the symbol signal-to-noise ratio, which is then used to assess the performance of the overall receiver. Quantifying the performance of the SSME, especially at high data rates, enables the user to determine the source of erroneous SNR measurements. These erroneous measurements may be attributed to the fundamental limitations of the SNR estimator or to the various tracking loops not being in-lock. This is particularly important for monitoring the symbol synchronization loop, as the only indication of its proper or improper operation is provided by the estimates of symbol SNR available from the SSME. In order to simplify the problem, it is assumed that the digital filter $H(z)$ is dominating and the effects of the analog filter are ignored. This is not the case in the ARX II, as both filters contribute equally. However, dealing with one filter will provide some insight into the behavior of the SSME in the presence of ISI.

A. Signal Model

Assuming that the carrier and subcarrier synchronization have been performed ideally, the baseband signal $r(t)$ can be modeled as

$$r(t) = \sqrt{(S)}d(t) + n(t) \tag{1}$$

where S is the data power and $d(t)$ denotes the actual data given by

$$d(t) = \sum_{n=-\infty}^{\infty} d_n p(t - nT) \tag{2}$$

where $p(t)$ is the baseband pulse limited to T sec (data rate $R = 1/T$) and d_n denotes the binary symbols ± 1. The additive noise $n(t)$ is zero-mean white Gaussian noise with two-sided power spectral density (PSD) $N_0/2$ watts/Hz. The continuous signal $r(t)$ is then sampled once every T_s seconds (sampling rate $f_s = 1/T_s$) to produce the sequence r_{ij}, as shown in Fig. 2. Consequently, the samples r_{ij} are given by

$$r_{ij} = \sqrt{(S)}d_{ij} + n_{ij} \tag{3}$$

where d_{ij} takes on the value ± 1 with equal likelihood and n_{ij} is a sequence of independent identically distributed zero mean Gaussian random variables with variance $N_0/2T_s$. The double subscript ij denotes the ith sample of the jth symbol. In this case the digital samples r_{ij} are then filtered by a general filter $H(z)$ to produce the string of samples y_{ij}, which form the input to the SSME. The digital filter $H(z)$ can be either a FIR or an IIR filter. In either case, the analysis to follow is applicable. Assume an integer number N_s of samples per symbol. This is a valid assumption when the sampling clock is controlled by the symbol synchronization loop to produce an even number of samples per symbol as in ARX I, (the previous version of the advanced receiver) [4]. However, in ARX II this is not the scenario, as the sampling clock is free running and is not synchronized with the symbol rate. As a result, the number of samples per symbol can change and hence, is not fixed. It is not the goal of this article to investigate the effects of noninteger samples per symbol on the performance of the SSME. Thus, only the integer number of samples per symbol case is considered. In writing Eq. (3), it is further assumed that the pulse $p(t)$ is an NRZ or a Manchester pulse. In either case, d_{ij} remains constant (1 or -1) for N_s or $N_s/2$ samples. By including an additional weighting factor, more general pulse shapes can also be accommodated. Note however that when the baseband pulse $p(t)$ contains nonzero rise or fall times due to analog filtering, the sampling offset (defined as the distance in time between the start of the pulse and the time at which the

first sample is taken) becomes an additional variable and should be considered in a performance prediction analysis.

B. The SSME Structure

In this section, the SSME is introduced and discussed briefly. Key performance parameters are also defined to evaluate the SSME performance in the presence of ISI. To the authors' knowledge, the SSME was first suggested by L. Howard [1] and later analyzed in white Gaussian noise by Simon and Mileant [2].

The SSME structure is depicted in Fig. 3. The upper "arm" sums the input samples y_{ij} over the first half of a symbol to produce $Y_{\alpha j}$, and the lower "arm" sums the input samples over the second half of a symbol to produce $Y_{\beta j}$. Subsequently, $Y_{\alpha j}$ and $Y_{\beta j}$ are first summed and squared to produce X_{ssj}, an estimate of total power, and secondly multiplied to yield X_{pj}, an estimate proportional to signal power. Next, X_{ssj} and X_{pj} are averaged over n symbols to obtain better estimates, namely, m_{ss} and m_p. Finally, m_p is appropriately weighted and subtracted from m_{ss} to obtain an estimate of noise power. This is then used with the signal power estimate to obtain an estimate of the symbol signal-to-noise ratio.

In order to evaluate the performance of the SSME, the SNR should be defined at various points in the system (see Fig. 2), in particular, the symbol SNR before the filter and the symbol SNR at the output of the filter which forms the input to the SSME. Obviously, it is expected that the SNR estimates of the SSME will coincide with the symbol SNR of the filtered signal, as the latter constitutes the input to the SSME. As the data rate is increased and the number of samples per symbol is reduced (assuming an approximately fixed sampling clock), it is expected that the SSME estimates will diverge from the symbol SNR; i.e., there is a data rate threshold above which the SSME breaks down.

The symbol SNR most commonly used in telecommunications is defined as the ratio of symbol energy E_s to the one-sided PSD level N_0, i.e., $SNR = E_s/N_0$. For rectangular symbols, $E_s = ST$. This can also be expressed in terms of the symbol noise variance as $SNR = S/2\sigma_n^2$ where $\sigma_n^2 = N_0/2T$. In terms of Fig. 2, this is the symbol SNR at the input to the filter. The symbol SNR at the output of the sum- and-dump filter, denoted by SNR' ($'$ denotes filtered), can be approximated by

$$SNR' \approx \frac{S'}{2\sigma_{n'}^2} \tag{4}$$

where S' and $\sigma_{n'}^2$ denote the average signal power and the noise variance at the output of the sum-and-dump filter, respectively. Equation (4) is an approximation because it does not include the "self noise" due to ISI (denoted σ_{ISI}^2) from adjacent symbols. An exact definition of SNR' would include σ_{ISI}^2 in the denominator of Eq. (4). However, in the case of low SNR, $\sigma_{n'}^2$ is much larger than σ_{ISI}^2, and the latter can be ignored. On the other hand, at high SNR, σ_{ISI}^2 dominates and Eq. (4) is invalid. In DSN applications, the signal is typically dominated by noise and not by ISI, hence, Eq. (4) is valid. Also note that the sum-and-dump filter is not a "true" matched filter. As a result, SNR' is not optimized. It is shown in Section I of the Appendix that SNR' as approximated in Eq. (4) can be expressed as

$$SNR' = \frac{S \sum_{k=-\infty}^{\infty} \left(\sum_{i=0}^{N_s-1} h_p(i+kN_s) \right)^2}{2 \sum_{i=0}^{N_s-1} \sum_{m=0}^{N_s-1} R_{n'}(i-m)} \tag{5}$$

where $h_p(i)$, $i = 0, 1, \ldots$, is the pulse response of the digital filter and $R_{n'}(k)$ is the autocorrelation function of the filtered noise $n'(m)$, defined by $R_{n'}(k) \triangleq E[n'(m)n'(m+k)]$. The indices of $h_p(\ )$ and $R_n(\ )$ correspond to sampling invervals. The double summation in the denominator accounts for the correlation between the ith noise sample and the mth noise sample of the same symbol. The summation over k in the numerator incorporates the contribution of ISI from all symbols. Strictly speaking, this sum is infinite for an IIR filter and finite for an FIR filter. In either case, the sum can be truncated to include only those symbols whose ISI contribution is significant. In the absence of filtering, $h(0) = 1$ and $h(i) = 0$ for $i \neq 0$. Consequently, the autocorrelation $R_{n'}(k) = (N_0/2T_s)[\delta(k) * h(k) * h(k)]$ simplifies to $(N_0/2T_s)\delta(k)$ and Eq. (5) reduces to ST/N_0, as expected.

C. The Performance of the SSME Algorithm

In this section, the performance of the SSME is evaluated in the presence of ISI. All results derived herein reduce to their counterpart for a wideband channel as in [2]. The input samples to the SSME are given by

$$y_{ij} = \sqrt{S} \sum_{m=-\infty}^{\infty} d_{j-m} h_p(i+mN_s) + n'_{ij} \tag{6}$$

159

where n'_{ij} are the filtered noise samples. We chose to represent y_{ij} in terms of the pulse response $h_p(n)$ to save the additional summation present when written in terms of the impulse response $h(n)$. In any case, $h_p(n)$ is related to the impulse response $h(n)$ via

$$h_p(n) = \sum_{m=0}^{N_s-1} h(n-m) \qquad (7)$$

From Fig. 2, the input samples y_{ij} are summed over the first half of a symbol to form the random variable $Y_{\alpha j}$; samples in the second half form $Y_{\beta j}$, i.e.,

$$Y_{\alpha j} = \sum_{i=0}^{(N_s/2)-1} y_{ij} \qquad (8a)$$

$$Y_{\beta j} = \sum_{i=N_s/2}^{N_s-1} y_{ij} \qquad (8b)$$

As discussed earlier, we form from the half-symbol accumulators the product and the sum squared of the outputs to get

$$X_{ssj} = (Y_{\alpha j} + Y_{\beta j})^2 \qquad (9a)$$

$$X_{pj} = Y_{\beta j} \cdot Y_{\alpha j} \qquad (9b)$$

These variables are the estimates of total power and signal power on a per symbol basis. To improve these estimates, we average over n symbols and obtain

$$m_{ss} = \frac{1}{n} \sum_{j=1}^{n} X_{ssj} \qquad (10a)$$

$$m_p = \frac{1}{n} \sum_{j=1}^{n} X_{pj} \qquad (10b)$$

Note that m_{ss} and m_p change at one nth of the data rate and n is a design parameter. Finally, an SNR estimate, SNR^*, is obtained by scaling and combining m_p and m_{ss} as follows:

$$SNR^* = \frac{m_p}{2\left(\frac{1}{4}m_{ss} - m_p\right)} \qquad (11)$$

Equation (11) describes the SSME SNR estimator which has been designed to operate in a wideband channel. Depending on its performance in the presence of ISI, modifications might be required to adopt the estimator for use in band-limited channels.

The mean and variance of SNR^* have been derived in [2] and are repeated below for convenience,

$$E[SNR^*] = \widehat{SNR} + \frac{1}{n}\left(1 + 2\widehat{SNR}\right) \qquad (12)$$

$$\text{Var}[SNR^*] = \frac{1}{n}\left(1 + 4\widehat{SNR} + 2\widehat{SNR}^2\right) \qquad (13)$$

where

$$\widehat{SNR} \triangleq \frac{E[m_p]}{2\left[\frac{1}{4}E[m_{ss}] - E[m_p]\right]} \qquad (14)$$

Equations (12) through (14) have been computed in the presence of AWGN and assume no ISI. Furthermore, they are approximate expressions which are valid for large n. Improved approximations could be obtained by retaining higher-order terms of the expansion as discussed in [3]. In the presence of filtering, these equations are not valid in the strict sense but can still serve as a guide, the quality of which is assessed via computer simulations at a later point. They are expected to be "good" approximations because we are operating in a noise-dominant rather than ISI-dominant scenario. It is shown in the Appendix that

$$E[m_p] = S \sum_{m=-\infty}^{\infty} \left[\sum_{i=0}^{(N_s/2)-1} h_p(i+mN_s) \cdot \sum_{k=N_s/2}^{N_s-1} h_p(k+mN_s) \right] + \sum_{i=0}^{(N_s/2)-1} \sum_{k=N_s/2}^{N_s-1} R_{n'}(i-k) \qquad (15a)$$

and

$$E[m_{ss}] = S \sum_{m=-\infty}^{\infty} \left[\sum_{i=0}^{N_s-1} h_p(i+mN_s) \right]^2 + \sum_{i=0}^{N_s-1} \sum_{k=0}^{N_s-1} R_{n'}(i-k) \qquad (15b)$$

which gives

$$\widehat{SNR} = \frac{S \sum_{m=-\infty}^{\infty} \left[\sum_{i=0}^{(N_s/2)-1} h_p(i+mN_s) \sum_{k=N_s/2}^{N_s-1} h_p(k+mN_s) \right] + \sum_{i=0}^{(N_s/2)-1} \sum_{k=N_s/2}^{N_s-1} R_{n'}(i,k)}{2\left[\frac{1}{4}\left(S \sum_{m=-\infty}^{\infty} \left[\sum_{i=0}^{N_s-1} h_p(i+mN_s) \right]^2 + \sum_{i=0}^{N_s-1} \sum_{k=0}^{N_s-1} R_{n'}(i,k) \right) - S \sum_{m=-\infty}^{\infty} \left(\sum_{i=0}^{(N_s/2)-1} h_p(i+mN_s) \sum_{k=N_s/2}^{N_s-1} h_p(k+mN_s) \right) - \sum_{i=0}^{(N_s/2)-1} \sum_{k=N_s/2}^{N_s-1} R_{n'}(i,k) \right]}$$

$$(16)$$

All these equations reduce to their respective counterparts in a wideband channel as in [2]. Namely, $E[m_p] = N_s^2 S/4, E[m_{ss}] = N_s^2 S + N_s N_0/2T_s$ and $\widehat{SNR} = ST/N_0$. Since the estimate SNR^* itself is a random variable, a measure of its quality is its signal-to-noise ratio given by

$$SNR(SNR^*) = \frac{E^2[SNR^*]}{\text{Var}[SNR^*]} \qquad (17a)$$

Using the approximations for $E[SNR^*]$ (Eq. 12), and Var$[SNR^*]$ (Eq. 13), one obtains

$$SNR(SNR^*) = \frac{\left[\widehat{SNR} + \frac{1}{n}\left(2\widehat{SNR} + 1 \right) \right]^2}{\frac{1}{n}\left(1 + 4\widehat{SNR} + 2\widehat{SNR}^2 \right)} \qquad (17b)$$

Note that in either limit, as SNR approaches 0 or ∞, one has

$$\widehat{SNR}_L = \frac{A_L}{2\left(\frac{1}{4}B_L - A_L \right)} \qquad L = 0, \infty \qquad (18)$$

where

$$A_0 = \sum_{i=0}^{(N_s/2)-1} \sum_{k=N_s/2}^{N_s-1} R_{n'}(i-k) \qquad (19a)$$

$$B_0 = \sum_{i=0}^{N_s-1} \sum_{k=0}^{N_s-1} R_{n'}(i-k) \qquad (19b)$$

$$A_\infty = S \sum_{m=-\infty}^{\infty} \left[\sum_{i=0}^{(N_s/2)-1} h_p(i+mN_s) \right.$$

$$\left. \times \sum_{k=N_s/2}^{N_s-1} h_p(k+mN_s) \right] \qquad (19c)$$

and

$$B_\infty = S \sum_{m=-\infty}^{\infty} \left[\sum_{i=0}^{N_s-1} h_p(i+mN_s) \right]^2 \qquad (19d)$$

and

$$\lim_{\text{SNR}\to L} SNR(SNR^*)$$

is given by Eq. (17b) with $\widehat{SNR}$ replaced by its respective limit. In the absence of filtering, $A_0 = 0$, $B_0 = (N_s N_0/2T_s)$, $A_\infty = (N_s/2)^2$ and $B_\infty = N_s^2$, which simplifies to

$$\lim_{SNR\to 0} SNR(SNR^*) = \frac{1}{n} \qquad (20a)$$

$$\lim_{SNR\to\infty} SNR(SNR^*) \simeq \frac{n}{2} + 2 \qquad (20b)$$

in agreement with [2]. Equations (18) and (19) depend on the filter $H(z)$ and cannot, in general, be simplified any further. Intuitively, however, $SNR(SNR^*)$ is expected to improve with n for high SNR even in the presence of ISI.

III. Numerical Results and Discussion

As mentioned earlier, the performance of the SSME needs to be assessed in the presence of ISI for various data rates. The digital filter used in the simulations is the half-band filter described in [5] with transfer function $H(z)$ given by

$$H(z) = -0.017 + 0.038z^{-2} - 0.089z^{-4}$$

$$+ 0.312z^{-6} + 0.5z^{-7} + 0.312z^{-8}$$

$$- 0.089z^{-10} + 0.038z^{-12} - 0.017z^{-14} \qquad (21)$$

and plotted in Fig. 4 versus normalized frequency. Note that the ratio of 3-dB bandwidth to sampling frequency is about 0.23. Assuming an effective sampling rate of 20 MHz (actual sampling rate is 40 MHz but telemetry processing at the output of the half-band filter is performed at 20 MHz due to decimation by two), the number of samples per symbol is given by $N_s = f_s T$. Thus, defining N_s is equivalent to specifying the data rate (for a fixed sampling rate). To get a feeling of the filtering involved, Fig. 5 depicts the pulse response and Fig. 6 shows a typical filtered sequence for $N_s = 2, 4, 10$ in the absence of noise. Note from Fig. 5 that a filtered pulse experiences interference from both past and future symbols due to the inherent filter delay.

The performance of the SSME in the presence of filtering is depicted in Fig. 8 versus the number of samples per symbol N_s. The figure shows analysis and simulation results for input SNRs of -5, 0, and 5 dB. As N_s decreases, the data rate increases and more ISI results. As N_s decreases below 6, SNR^* diverges from SNR' and the SSME breaks down. Surprisingly, the estimated SNR^* are several decibels higher than SNR' in the breakdown region. However, it is unclear whether the divergence of the estimates is due to the ISI or colored noise. In order to gain more insight into the causes, the effects of ISI and colored noise are considered separately. Figures 10 and 12 depict the SSME response when the data or the noise are filtered, but not both. When the data is filtered (Fig. 10), the estimated SNR, denoted by SNR_d^*, is still valid even for $N_s < 6$. In this special scenario, Eqs. (5) and (16) reduce to give

$$SNR_d' = \frac{S \sum_{k=-\infty}^{\infty} \left(\sum_{i=0}^{N_s-1} h_p(i + kN_s) \right)^2}{2N_s^2 \sigma_n^2} \qquad (22a)$$

and

$$\widehat{SNR}_d = \frac{S \sum_{m=-\infty}^{\infty} \left[\sum_{i=0}^{(N_s/2)-1} h_p(i + mN_s) \sum_{k=N_s/2}^{N_s-1} h_p(k + mN_s) \right]}{2\left[\frac{1}{4}\left(S \sum_{m=-\infty}^{\infty} \left[\sum_{i=0}^{N_s-1} h_p(i + mN_s) \right]^2 \right) + N_s^2\sigma_n^2 - \sum_{m=-\infty}^{\infty} \left(\sum_{i=0}^{(N_s/2)-1} h_p(i + mN_s) \sum_{k=n_s/2}^{N_s-1} (k + mN_s) \right) \right]} \qquad (22b)$$

The subscript d is to indicate that only the data is filtered. Both equations are shown in Fig. 10 along with simulation points. As N_s decreases, SNR'_d and SNR^*_d decrease because more signal energy is lost due to filtering. Also note that at $N_s = 2$, SNR^* and SNR' coincide better at low SNR and they diverge for high SNR. The curvature of the graph in Fig. 10 is opposite to that of Fig 8. That tends to indicate that ISI itself is not the reason why SNR^* of Fig. 8 increases for low N_s. This phenomenon is better explained by Fig. 12, which depicts the SSME response in the presence of correlated noise, but unfiltered data. In that case, Eqs. (5) and (16) simplify to

$$SNR'_n = \frac{SN_s^2}{2 \displaystyle\sum_{i=0}^{N_s-1} \sum_{m=0}^{N_s-1} R_{n'}(i-m)} \tag{23a}$$

$$\widehat{SNR}_n = \frac{\dfrac{SN_s^2}{4} + \displaystyle\sum_{i=0}^{(N_s/2)-1} \sum_{k=N_s/2}^{N_s-1} R_{n'}(i-k)}{2\left[\dfrac{1}{4}\left(SN_s^2 + \displaystyle\sum_{i=0}^{N_s-1}\sum_{k=0}^{N_s-1} R_{n'}(i-k)\right) - \dfrac{SN_s^2}{4} - \displaystyle\sum_{i=0}^{N_s/2}\sum_{k=N_s/2}^{N_s-1} R_{n'}(i-k)\right]} \tag{23b}$$

where the subscript n indicates that only noise is filtered. For $N_s < 6$, the SSME seems to break down due to noise correlation. Recall that the SSME estimates noise power by subtracting signal power estimate from total power estimate. The signal power estimate X_{pj} (see Fig. 3) is formed by the product of the accumulator outputs. In the absence of filtering, that product contains independent noise samples whose effect is reduced by averaging over n symbols. In the presence of filtering and specifically for low N_s, the noise samples in that product are highly correlated and contribute to the signal power estimate even after averaging. That in turn reduces the noise power estimate after subtracting from the estimate of total power, hence significantly increasing SNR^*_n. Obviously, the noise correlation also increases the total power estimate but that increase is still less than its counterpart in estimating signal power, taking into account the appropriate weighting. In Figs. 13 and 14, SNR^* is plotted versus SNR (Fig. 13) and SNR' (Fig. 14) for a fixed N_s when both the data and noise are filtered. As expected, a linear relationship is obtained for large values of N_s and a nonlinear relationship as the data rate increases.

Finally, as an indication of the quality of the estimates, Figs 15 and 16 depict $SNR(SNR^*)$ versus SNR for a fixed N_s (Fig.15) and fixed n (Fig. 16). As more symbols are used to provide an SNR estimate, an improved performance is expected and this is clearly shown in Fig. 15. From Fig. 16, it is also clear that $SNR(SNR^*)$ improves with decreasing N_s. This is a rather surprising result at first glance. But remember that $SNR(SNR^*)$ is an indication of how the estimate jitters about its mean, no matter where the mean is. Also recall that for $N_s = 4$ the definition of SNR in Eq. (4) is invalid as the variance due to ISI might be significant. The simulations were conducted using 25,000 symbols for $N_s \geq 10$ and 50,000 symbols for $N_s < 10$, with varying n depending on the SNR.

IV. Conclusion

This article deals with the performance of the SSME in the presence of ISI, evaluated both analytically and by simulation. It is shown that the estimator performs well with more than 6 samples per symbol, but poorly with fewer than 6 samples per symbol due to the high correlation among noise samples of the same symbol. Further work would be required to reduce the bias in the estimates that occur with few samples per symbol.

References

[1] L. D. Howard, "Signal and Noise Measurements in the NASA Deep Space Network," *20th URSI Conference*, Washington, D.C., August 10–19, 1981.

[2] M. K. Simon and A. Mileant, "SNR Estimation for the Baseband Assembly," *TDA Progress Report 42-85*, vol. January–March 1986, Jet Propulsion Laboratory, Pasadena, California, pp. 118–126, May 15, 1986.

[3] M. G. Kindel and A. Stuart, *The Advanced Theory of Statistics*, vol. I, New York: Hafner Publishing Co., 1973.

[4] D. H. Brown and W. J. Hurd, "DSN Advanced Receiver: Breadboard Description and Test Results," *TDA Progress Report 42-89*, vol. January–March 1987, Jet Propulsion Laboratory, Pasadena, California, pp. 48–66, May 15, 1987.

[5] R. Sadr and W. J. Hurd, "Digital Carrier Demodulation for the DSN Advanced Receiver," *TDA Progress Report 42-93*, vol. January–March 1988, Jet Propulsion Laboratory, Pasadena, California, pp. 45–63, May 15, 1988.
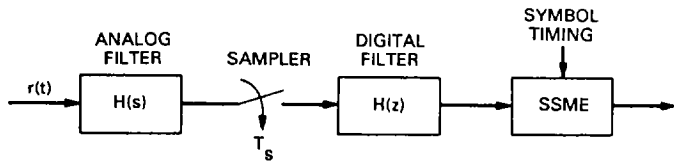
Fig. 1. General signal processing model.
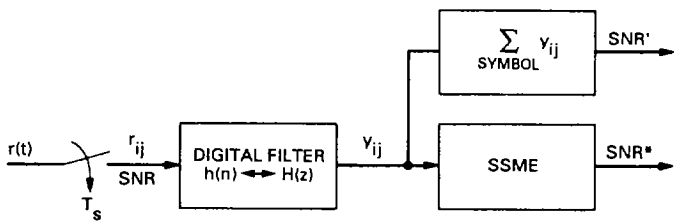
Fig. 2. Signal model.
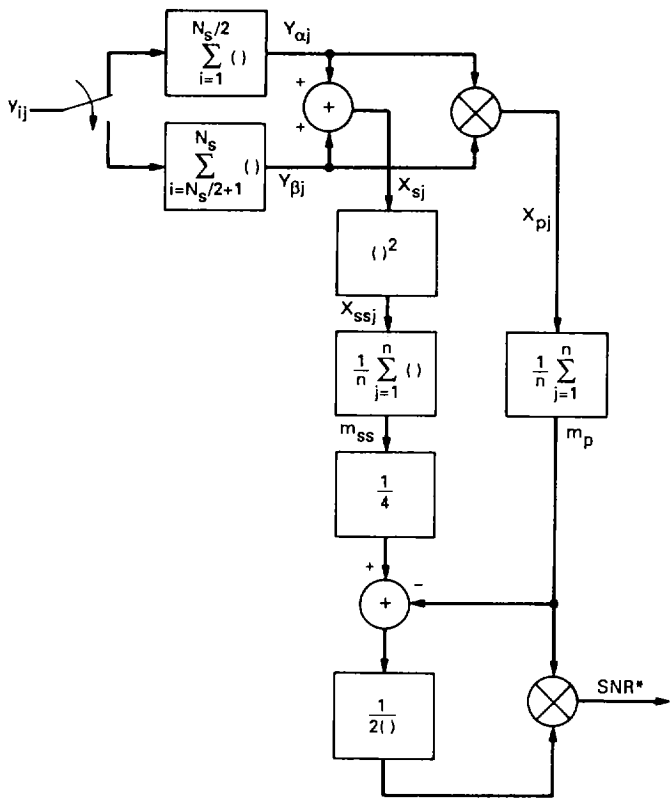
Fig. 3. The SSME structure.
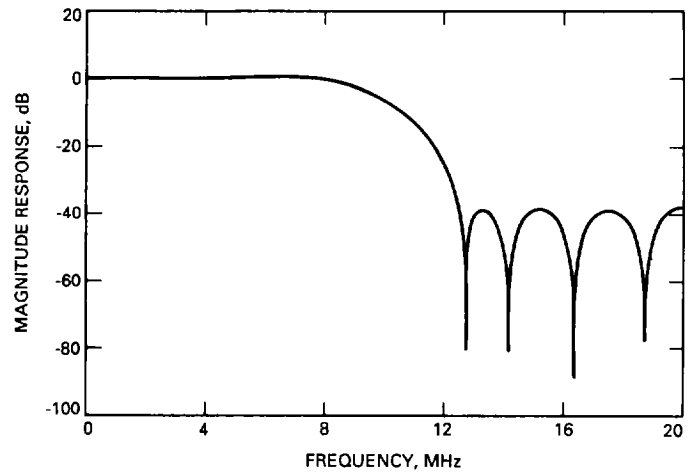
Fig. 4. Digital filter frequency response (20-MHz processing rate).
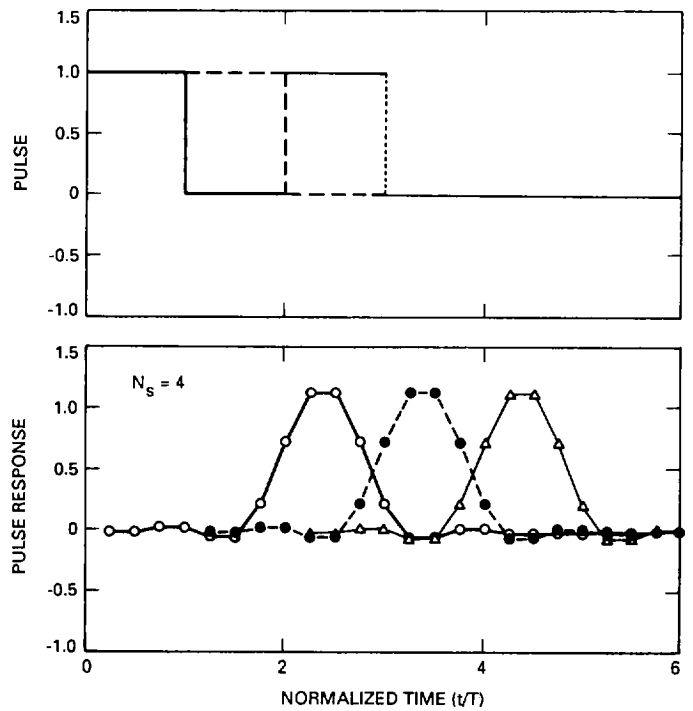
Fig. 5. Pulse response of the half-band filter.
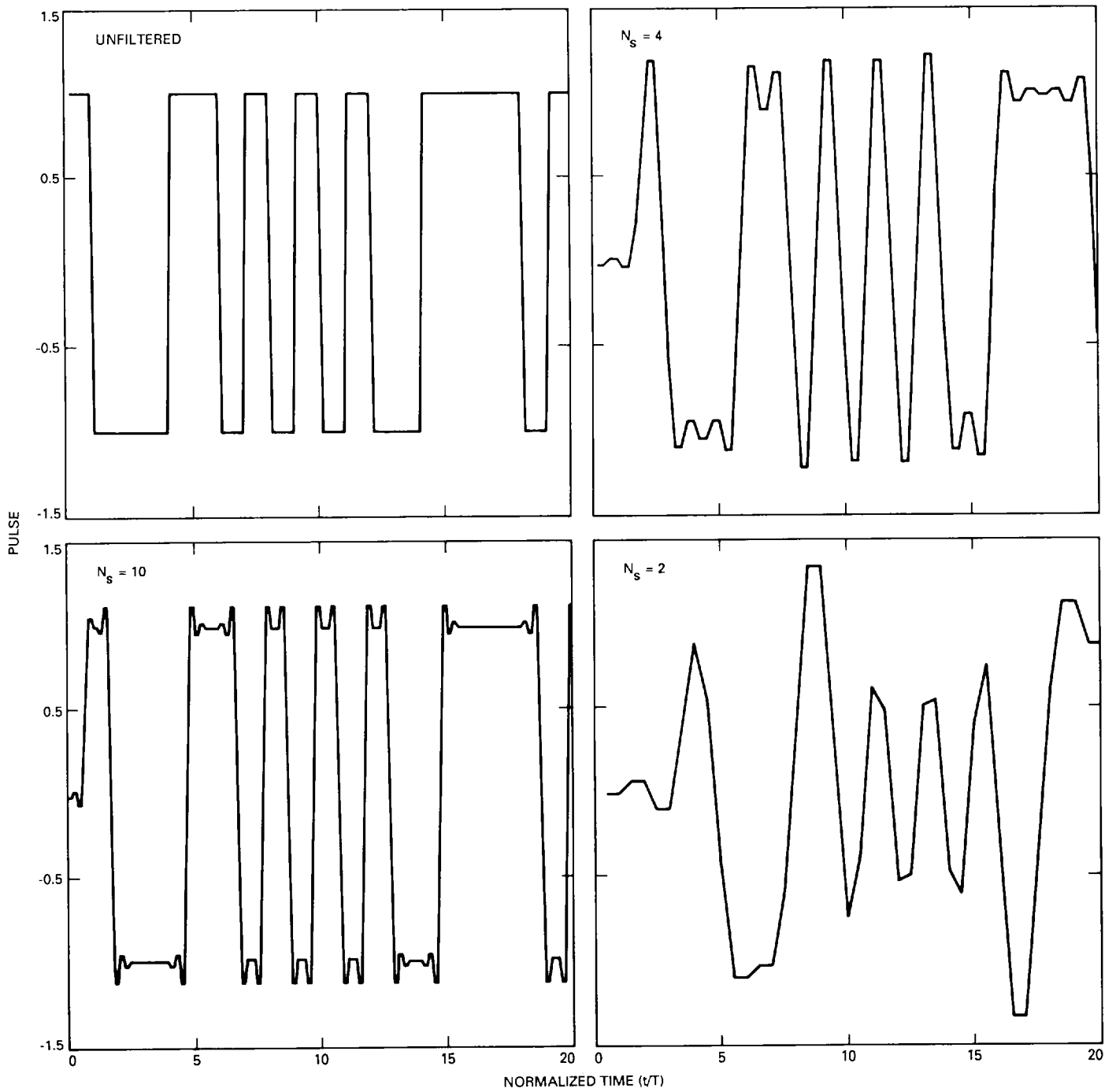
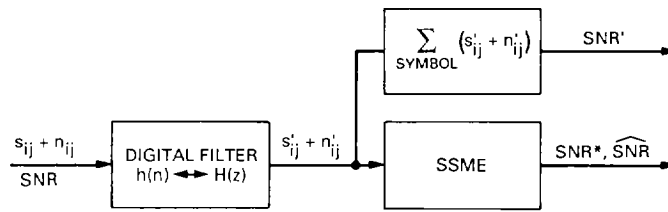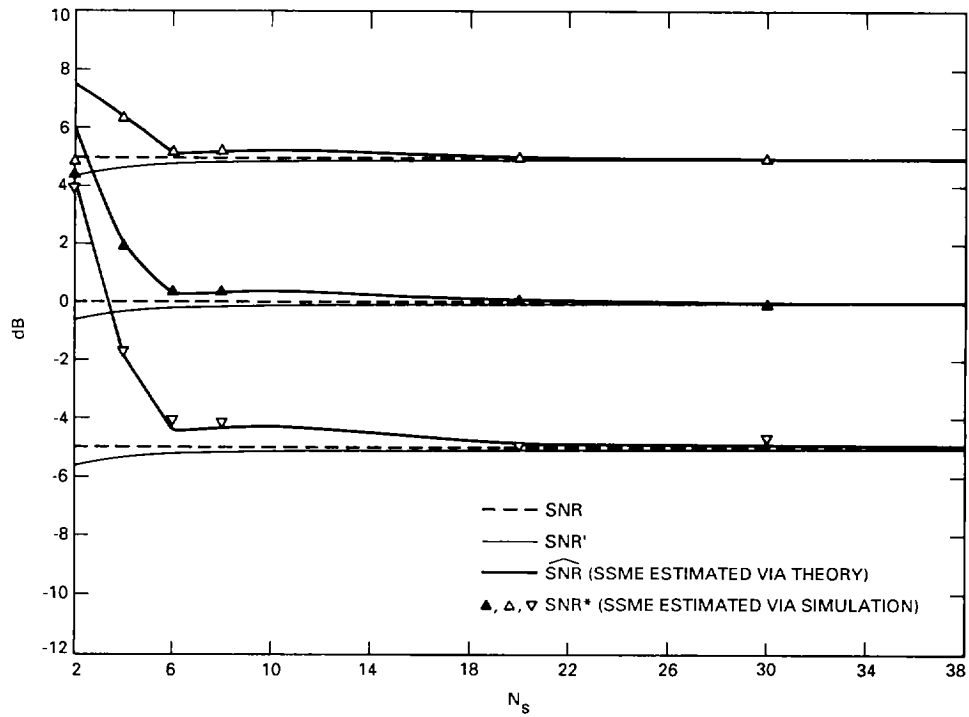**Fig. 6. Filtered data sequences for $N_s = 2, 4, 10$.**

Fig. 7. System model for Fig. 8.

Fig. 8. SNR, SNR', SNR*, and $\widehat{SNR}$ versus N_s (data and noise filtered).
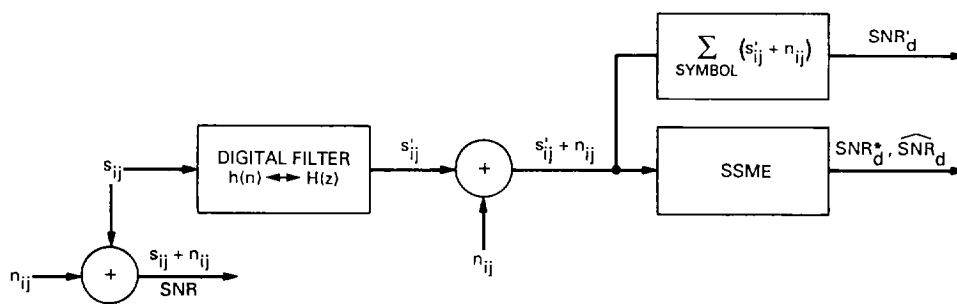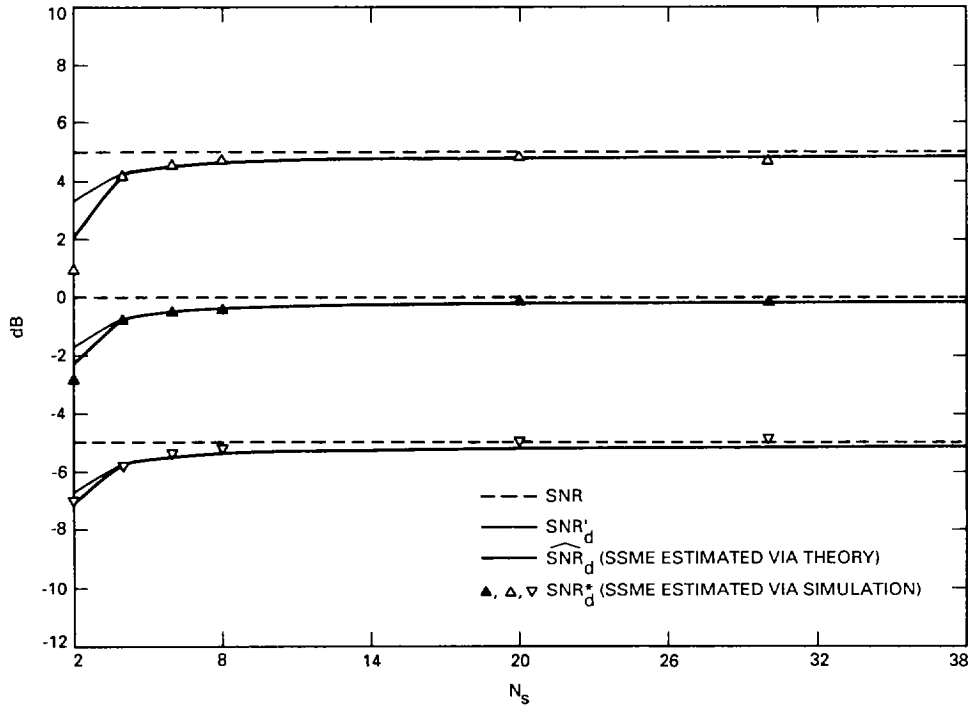

Fig. 9. System model for Fig. 10.

Fig. 10. SNR, SNR$_d'$ and $\widehat{SNR}_d$ versus N_s (data filtered).
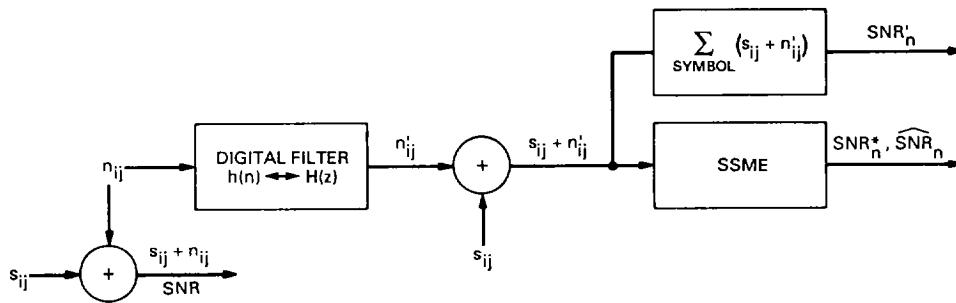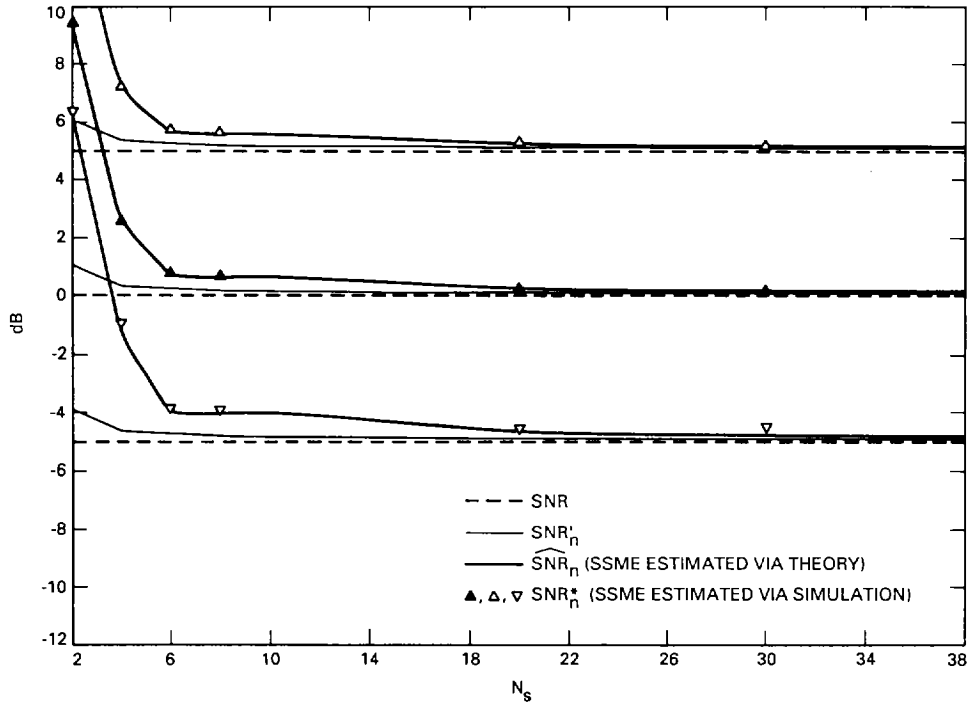

Fig. 11. System model for Fig. 12.

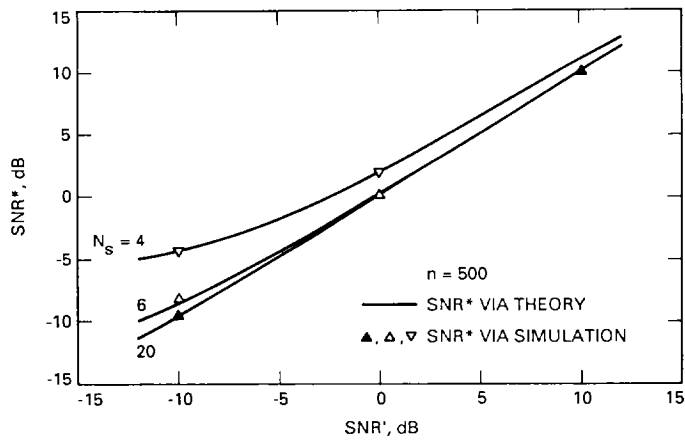**Fig. 12. SNR, SNR'$_n$, and $\widehat{SNR}_n$ versus N$_s$ (noise filtered).**

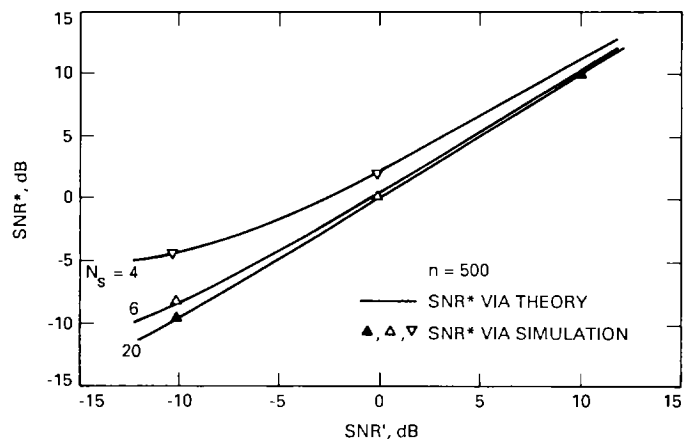

Fig. 13. SNR* versus SNR (data and noise filtered).
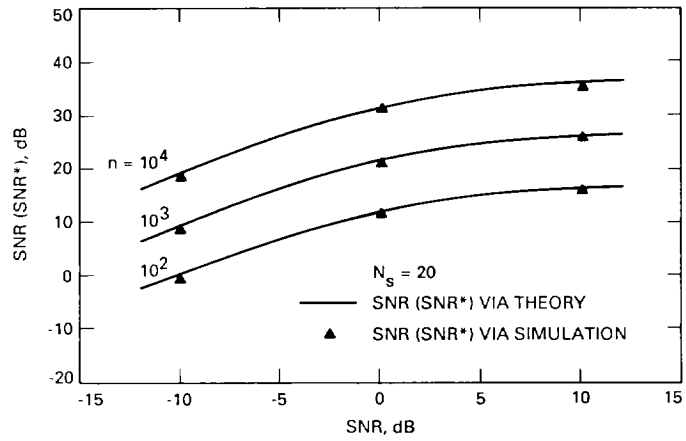

Fig. 14. SNR* versus SNR' (data and noise filtered).
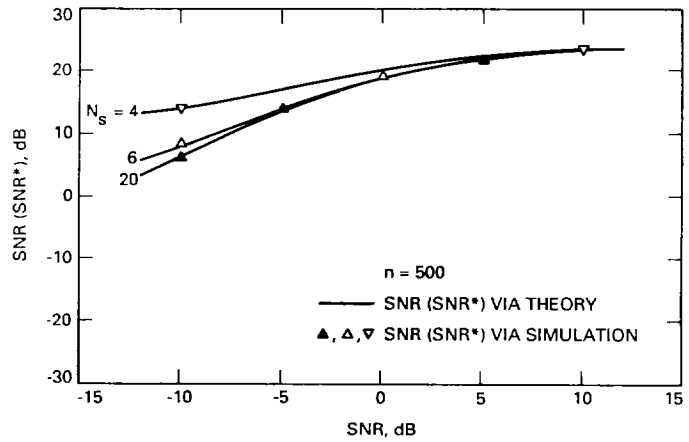
Fig. 15. SNR(SNR*) versus SNR (fixed N_s, varying n).

Fig. 16. SNR(SNR*) versus SNR (varying N_s, fixed n).

Appendix
Derivation of Equations

I. Derivation of Equation (5)

The approximate symbol signal-to-noise ratio at the output of the digital filter, SNR', is given by

$$SNR' = \frac{S'}{2\sigma_{n'}^2} \qquad \text{(A-1)}$$

where S' and $\sigma_{n'}^2$ denote the average signal power and the noise variance respectively at the output of the sum-and-dump filter. We begin our derivation of the signal power in the filtered symbol with an expression for the ith sample of the jth filtered symbol, y_{ij}. Namely,

$$y_{ij} = \sqrt{S}\Big[d_j h_p(i) + d_{j-1}h_p(i+N_s)$$

$$+ d_{j-2}h_p(i+2N_s)\Big] + \cdots + n'_{ij}$$

$$i = 0, 1, 2, \ldots, N_s - 1$$

$$= \sqrt{S}\sum_{m=-\infty}^{\infty} d_{j-m}h_p(i+mN_s) + n'_{ij}$$

$$i = 0, 1, 2, \ldots, N_s - 1 \quad \text{(A-2)}$$

where d_j is the jth received symbol, $h_p(i)$ is the pulse response at time i, and n'_{ij} is the noise sample at the output

of the digital filter. Let s'_{ij} be the signal portion of y_{ij}. Clearly then,

$$s'_{ij} = \sqrt{S}\sum_{m=-\infty}^{\infty} d_{j-m}h_p(i+mN_s) \quad i = 0, 1, 2, \ldots, N_s - 1$$

$$\text{(A-3)}$$

and the signal power, S', is

$$S' = E\left[\left(\sum_{i=0}^{N_s-1} s'_{ij}\right)^2\right]$$

$$\text{(A-4)}$$

where $E[\ ]$ is the expected value operator to average over the random data. Substituting Eq. (A-3) into Eq. (A-4) yields

$$S' = E\left[\left(\sqrt{S}\sum_{i=0}^{N_s-1}\sum_{m=-\infty}^{\infty} d_{j-m}h_p(i+mN_s)\right)^2\right]$$

Separating the above equation into four sums and moving the expected value operator inside the summations yields:

$$S' = S\sum_{i=0}^{N_s-1}\sum_{\ell=0}^{N_s-1}\sum_{m=-\infty}^{\infty}\sum_{n=-\infty}^{\infty} E[d_{j-m}d_{j-n}]h_p(i+mN_s)h_p(\ell+nN_s) = S\sum_{n=-\infty}^{\infty}\left[\left(\sum_{i=0}^{N_s-1} h_p(i+nN_s)\right)^2\right] \qquad \text{(A-5)}$$

where the last step follows since $E[d_{j-n}d_{j-m}] = \delta(n - m)$ for all j. Using Eq. (7), S' can be expressed in terms of the impulse response as

$$S' = S \sum_{n=-\infty}^{\infty} \left[\left(\sum_{i=0}^{N_s-1} \sum_{m=0}^{N_s-1} h(i + nN_s - m) \right)^2 \right] \quad (A-6)$$

The filtered noise variance $\sigma_{n'}^2$, on a per symbol basis, is defined as the expected value of the squared sum of N_s noise samples, i.e.,

$$\sigma_{n'}^2 = E\left[\left(\sum_{i=0}^{N_s-1} n'_{ij} \right)^2 \right] = \sum_{i=0}^{N_s-1} \sum_{\ell=0}^{N_s-1} R_{n'}(i - \ell) \quad (A-7)$$

where $R_{n'}(m)$ is the autocorrelation function of the filtered noise samples. Using Eqs. (A-5) and (A-7) in Eq. (A-1),

$$SNR' = \frac{S \displaystyle\sum_{n=-\infty}^{\infty} \left[\left(\displaystyle\sum_{i=0}^{N_s-1} h_p(i + nN_s) \right)^2 \right]}{2 \displaystyle\sum_{i=0}^{N_s-1} \sum_{\ell=0}^{N_s-1} R_{n'}(i - \ell)} \quad (A-8)$$

II. The Expected Value of X_{ss}, X_p, m_{ss}, and m_p

As indicated in Fig. 3, the random variable X_{ssj} is the squared sum of N_s input samples. Hence, the expected value of X_{ssj} is

$$E[X_{ssj}] = E\left[\left(\sum_{i=0}^{N_s-1} y_{ij} \right)^2 \right] \quad (A-9)$$

Substituting for y_{ij} from Eq. (A-2) in Eq. (A-9) gives

$$E[X_{ssj}] = E\left[\sqrt{S} \sum_{i=0}^{N_s-1} \left(\sum_{m=-\infty}^{\infty} d_{j-m}h_p(i + mN_s) + n'_{ij} \right) \right]^2 \quad (A-10)$$

Carrying out the square in the above equation, moving the expectation operator through the summations, and noting the following: $E[a_{j-m}a_{j-\ell}] = \delta(m - \ell)$ for all j, $E[a_{j-m}n'_{ij}] = 0$ for any i, j, and m, and $E[n'_{ij}n'_{kj}] = R_{n'}(i - k)$ for all j, the desired result is obtained, namely,

$$E[X_{ssj}] = S \sum_{m=-\infty}^{\infty} \left[\sum_{i=0}^{N_s-1} h_p\left(i + mN_s\right) \right]^2$$

$$+ \sum_{i=0}^{N_s-1} \sum_{k=0}^{N_s-1} R_{n'}(i - k) \quad (A-11)$$

Note that $E[X_{ssj}]$ is independent of j and henceforth the subscript j can be dropped from $E[X_{ssj}]$ and the expected value of X_{ssj} can be denoted by $\overline{X}_{ss}$. As shown in Fig. 3, the random variable X_{pj} is the product of the sum of samples from the first half of a symbol with the sum of samples from the second half of a symbol. Consequently, the expected value of X_{pj} is given as

$$E[X_{pj}] = E\left[\sum_{i=0}^{(N_s/2)-1} y_{ij} \sum_{k=N_s/2}^{N_s-1} y_{kj} \right] \quad (A-12)$$

Substituting for y_{ij} from Eq. (A-2),

$$E[X_{pj}] = E\left[S \sum_{i=0}^{(N_s/2)-1} \left(\sum_{m=-\infty}^{\infty} d_{j-m}h_p(i + mN_s) + n'_{ij} \right) \sum_{k=N_s/2}^{N_s-1} \left(\sum_{\ell=-\infty}^{\infty} d_{j-\ell}h_p(k + \ell N_s) + n'_{ij} \right) \right] \quad (A-13)$$

Expanding the product in the equation above and taking the expectation of the received data symbols, filtered noise, as well as the product of data and noise yields the desired result:

$$E[X_{pj}] = S \sum_{m=-\infty}^{\infty} \left[\sum_{i=0}^{(N_s/2)-1} h_p(i + mN_s) \sum_{k=N_s/2}^{N_s-1} h(k + mN_s) \right] + \sum_{i=0}^{(N_s/2)-1} \sum_{k=N_s/2}^{N_s-1} R_{n'}(i-k) \qquad \text{(A-14)}$$

Note that $E[X_{pj}]$ is independent of j and henceforth the subscript j can be dropped from $E[X_{pj}]$ and the expected value of X_{pj} can be denoted by $\overline{X}_p$. The random variables m_{ss} and m_p are formed by scaling and summing the random variables X_{ssj} and X_{pj} over n symbols. Consequently, the expected values of m_{ss} and m_p are the expected values of these scaled sums. But, since $E[X_{ssj}]$ and $E[X_{pj}]$ are constant from symbol to symbol (i.e., independent of j),

$$E[m_{ss}] = \overline{X_{ss}} \qquad \text{(A-15a)}$$

and

$$E[m_p] = \overline{X_p} \qquad \text{(A-15b)}$$